Journal of
Mechanics of
Materials and Structures

BUCKLING AND POSTBUCKLING BEHAVIOR OF LAMINATED COMPOSITE STRINGER STIFFENED CURVED PANELS UNDER AXIAL COMPRESSION: EXPERIMENTS AND DESIGN GUIDELINES

Haim Abramovich and Tanchum Weller

Volume 4, Nº 7-8 September 2009

mathematical sciences publishers

JOURNAL OF MECHANICS OF MATERIALS AND STRUCTURES
Vol. 4, No. 7-8, 2009

BUCKLING AND POSTBUCKLING BEHAVIOR OF LAMINATED COMPOSITE STRINGER STIFFENED CURVED PANELS UNDER AXIAL COMPRESSION: EXPERIMENTS AND DESIGN GUIDELINES

HAIM ABRAMOVICH AND TANCHUM WELLER

An extensive test series on circular cylindrical laminated composite stringer-stiffened panels subjected to axial compression, shear loading introduced by shear and combined axial compression and shear was carried out at the Technion, Israel. The test program was an essential part of an ongoing effort undertaken by the POSICOSS project (improved postbuckling simulation for design of fibre composite stiffened fuselage structures) aiming at design of low cost, low weight airborne structures that was initiated and supported by the Fifth European Initiative Program.

The first part of this test series, dealing with panels PSC1–PSC9 (blade-stiffened), has already been summarized and published. The results of the tests with panels BOX1–BOX4 (blade- and J-stiffened) have also been reported and published. These tests dealt with two identical stiffened panels, combined together by two flat nonstiffened aluminum webs, to form a torsion box, thus enabling application of shear tractions, through introduction of torsion, and combined axial compression and shear. The present manuscript aims at describing test results and relevant numerical studies on the buckling and postbuckling behavior of another set of four panels, AXIAL1–AXIAL4, stiffened by J-type stringers. Based on the experimental studies carried out within the framework of the POSICOSS project and reported in the literature and on the present study design guidelines were formulated and presented. Accompanying supporting calculations were presented as well; they were performed with a "fast" calculation tool developed at the Technion, and based on the effective width method modified to handle laminated circular cylindrical stringer-stiffened composite panels.

1. Introduction

It is well recognized that non-closely stiffened panels can have considerable postbuckling reserve strength, enabling them to carry loads significantly in excess of their initial local skin between stiffeners buckling load [Hutchinson and Koiter 1970]. When appropriately designed, their load carrying capacity appreciably exceed the load corresponding to an equivalent weight unstiffened shell, that is, a shell of identical radius and thicker skin, which is also more sensitive to geometrical imperfections.

The design of aerospace structures places great emphasis on exploiting the behavior under loading and on mass minimization of such panels. An optimum (minimum mass) design approach based on initial buckling, stress or strain, and stiffness constraints typically yields an idealized structural configuration characterized by almost equal critical loads for local and overall buckling. This, of course, results in little

This work was partly supported by the European Commission, Competitive and Sustainable Growth Programme, Contract No. G4RD-CT-1999-00103, project POSICOSS (http://www.posicoss.de). The information in this paper is provided as is and no guarantee or warranty is given that the information is fit for any particular purpose. Users thereof use the information at their sole risk and liability.

postbuckling strength capacity and susceptibility to premature failure. However, an alternative optimum design approach can be imposed to achieve lower mass designs for a given loading. This is obtained by requiring the initial local buckling to occur considerably below the design load and allow for the existence of the response characteristics known in postbuckled panels [Lilico et al. 2002], that is, capability to carry loads higher than their initial buckling load. In parallel, to meet the requirements of low structure weight, advanced lightweight laminated composite elements are increasingly being introduced into new designs of modern aerospace structures to enhance both their structural efficiency and performance. In recognition of the numerous advantages that such composites offer, there is also a steady growth in replacement of metallic components by composite ones in other fields of engineering like marine structures, ground transportation, robotics, sports, and others.

Many theoretical and experimental studies have been performed on buckling and postbuckling behavior of flat stiffened composite panels (see for example [Frostig et al. 1991; Segal et al. 1987; Starnes et al. 1985; Vestergen and Knutsson 1978; Romeo 1986; Bucci and Mercuria 1992]). A wide body of descriptions and detailed data on buckling and postbuckling tests was compiled in [Singer et al. 2002] (see chapters 12–14). However, on the other hand studies on cylindrical, unstiffened, and stiffened composite shells and curved unstiffened and stiffened composite panels were quite scarce (see for example [Lei and Cheng 1969; Johnson 1978; Tennyson et al. 1972; Card 1966; Knight and Starnes 1988; Sobel and Agarwal 1976]) at the starting time of the POSICOSS project [Zimmermann and Rolfes 2006] and later its successor, the COCOMAT project [Degenhardt et al. 2006].

In light of the above discussion, in compliance with the demand of the Fifth European Initiative Program to reduce weight without prejudice to cost and structural life in design of next generation aircraft[1], and in recognition of the advantages inherent to post buckled stiffened structures, it has been suggested to asses the introduction of buckled structures and allow buckling in operation of fuselage structures under ultimate load levels. This approach has been adopted and undertaken in the present experimental study, the POSICOSS project. It was particularly aimed at supporting the development of improved, fast and reliable procedures for analysis and simulation of postbuckling behavior of fiber reinforced composite circular cylindrical stiffened panels of future generation fuselage structures and their design.

Within the POSICOSS project, the Aerospace Structures Laboratory (ASL) at the Technion – Israel Institute of Technology performed an extensive test series on the above mentioned type laminated composite stringer-stiffened panels under axial compression, shear loading introduced by torsion, and combined axial compression and shear. The buckling and postbuckling behavior of these panels was recorded till their final collapse and the test results were analyzed and compared with calculated predictions. The first part of this test series, dealing with panels stiffened by blade type stringers (PSC1–PSC9), was summarized in [Abramovich et al. 2003]. The results of the tests with panels stiffened by blade type stringers or J-type stringers (BOX1–BOX4) were reported in [Abramovich et al. 2008]. These tests deal with two identical panels, combined together by two flat nonstiffened aluminum webs, to form a torsion box, thus enabling application of shear tractions through introduction of torsion, as well as combined axial compression and shear. The present manuscript aims at describing and evaluating the buckling

[1]This design approach was summarized by the specialists of the European Community in the year 2000 under the name Vision 2020. It can be found at the EU website http://cordis.europa.eu

and postbuckling behavior of test results and relevant numerical studies of another set of four panels, AXIAL1–AXIAL4, stiffened by J-type stringers. Based on the results of the experimental study carried out within the framework of the POSICOSS project and reported in [Abramovich et al. 2003; 2008] and the present manuscript, and employing the "fast" tool of [Pevzner et al. 2008] to calculate the collapse loads of the axially compressed panels, design guidelines were formulated and presented.

2. Specimens and test setup

Within the framework of the POSICOSS effort, Israel Aircraft Industries (IAI) has designed and manufactured 21 Hexcel IM7 (12 K) / 8552(33%) graphite-epoxy stringer-stiffened composite circular cylindrical panels using a cocuring process. Adhering to the goal of POSICOSS, namely low weight low cost structures, simple blade and J-type stringers were employed to stiffen the panels. The nominal radius of each panel was $R = 938$ mm and its total length $L = 720$ mm (which included two end loading pieces each 30 mm high). The nominal test length was $L_n = 680$ mm and the panel arc-length was $L_{al} = 680$ mm. The skin lay-up was quasiisotropic $(0°, \pm 45°, 90°)_S$. Each layer had a nominal thickness of 0.125 mm. Eight of these panels were used to form 4 torsion boxes. Each box consisted of two curved panels that were connected together by two flat nonstiffened aluminum side plates. Two of the boxes comprised of panels with blade type stringers (Figure 1, top), one box had short-flange J-type stringers (Figure 1, middle) and the fourth box had long-flange J-type stringers (Figure 1, bottom). The dimensions and properties of the different configurations are shown in these figures. The results of the tests experienced with these boxes and corresponding calculations were reported in [Abramovich et al. 2008]. Nine out of these panels, PSC1–PSC9, stiffened by blade type stringers (Figure 1, top) were tested under axial compression and the relevant test results and calculations were reported in [Abramovich et al. 2003]. The last four panels designated as AXIAL1–AXIAL4 with J-type stringers, which are presented in the middle and bottom parts of Figure 1, were tested under axial compression. The test results and numerical studies associated with them are presented in what follows.

It is seen on Table 1 that the two panels AXIAL1 and AXIAL2 were stiffened by five stringers, while AXIAL3 and AXIAL4 had four stringers. The four panels were tested under axial compression only using the 50 tons MTS loading machine at the Aerospace Structures Laboratory, Faculty of Aerospace Engineering, Technion – Israel Institute of Technology, Haifa, Israel (Figure 2).

To visualize the development of displacements and buckling patterns, the Moiré technique has been applied [Abramovich et al. 2003; 2008]. To monitor and record the panel response due to application of axial compression, strain gages were bonded back-to-back, both on the skin and on the stringers. Lateral and axial LVDTs were used to record the out-of-plane deflections and the end-shortening (Figures 3 and 8).

3. Experimental results

The first panel tested was AXIAL1. First buckling occurred at 85 kN near gage #24 close to the upper loading end piece (Figure 3). Increase in axial compression caused the appearance of more buckling waves (see typical behavior in the first three parts of Figure 4). Typical strain gage readings (gages #27 and 28) at panel mid-height close to the panel supported unloaded edge (see Figure 3) are shown in Figure 5, top, where buckling is apparent at about 87 kN. For comparison, readings for strain gages

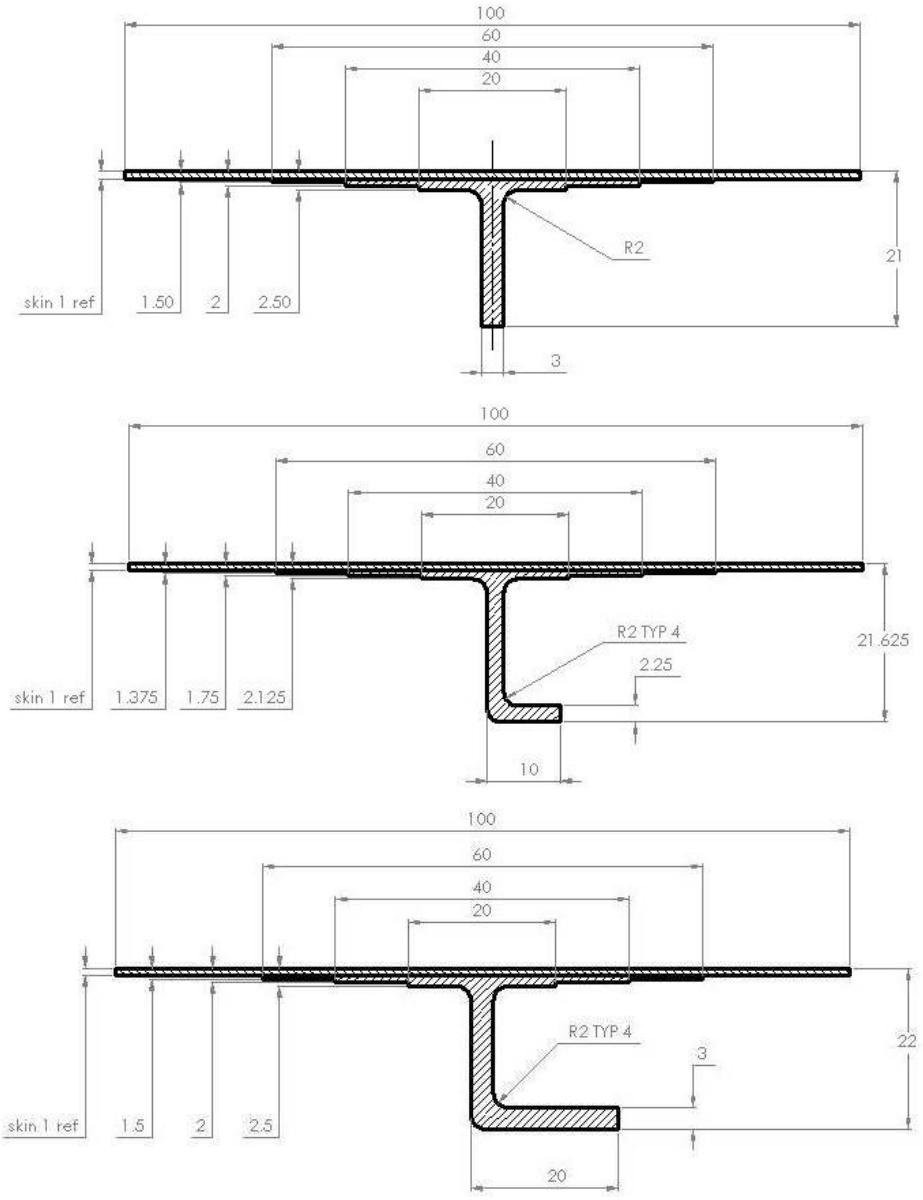

Figure 1. Dimensions, geometry and lay-ups of stiffeners. Top: Panels PSC1–PSC9 [Abramovich et al. 2003], BOX1 and BOX2 [Abramovich et al. 2008]. Middle: Panels AXIAL1, AXIAL2, and BOX 3 [Degenhardt et al. 2006]. Bottom: Panels AXIAL3, AXIAL4, and BOX4 [Abramovich et al. 2008].

#23 and 24 are displayed in Figure 5, bottom. The buckling is observed under slightly a lower load of about 80 kN. A fully developed pattern of buckling waves was obtained under 173 kN. The axial loading was increased till 229.88 kN, when a delamination occurred near strain gage #4 (Figure 3), between the skin and the stringer. Following the occurrence of the delamination, the load dropped to 224.5 kN. The

	Stringer type	
	Short-flange J	Long-flange J
Specimens	AXIAL1, AXIAL2	AXIAL3, AXIAL4
Total panel length	720 mm	720 mm
Free panel length	660 mm	660 mm
Radius	938 mm	938 mm
Arc length	680 mm	680 mm
Number of stringers	5	4
Stringer spacing	136 mm	174 mm
Laminate lay-up of skin	$[0, 45, -45, 90]_s$	$[0, 45, -45, 90]_s$
Laminate lay-up of stringer	$[45, -45, 0]_{3s}$	$[45, -45, 0_2]_{3s}$
Ply thickness	0.125 mm	0.125 mm
Type of stringer	J-stringer	J-stringer
Stringer height	20.5 mm	20.5 mm
Stringer feet width	60 mm	60 mm
Stringer flange width	10 mm	20 mm
E_{11}	147300 N/mm^2	147300 N/mm^2
E_{22}	11800 N/mm^2	11800 N/mm^2
G_{12}	6000 N/mm^2	6000 N/mm^2
ν_{12}	0.3	0.3

Table 1. Dimensions, lay-ups and mechanical properties used in calculations of load carrying capacity panels AXIAL1–AXIAL4 (present study).

Figure 2. Panel in loading machine setup used at the Aerospace Structures Laboratory (ASL).

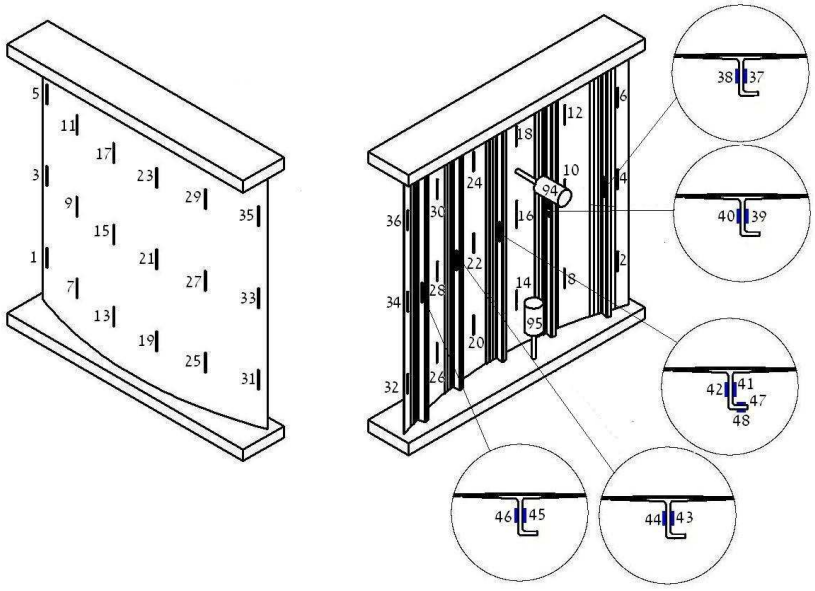

Figure 3. Locations of strain gages and axial and lateral LVDT's for panels AXIAL1 and AXIAL2.

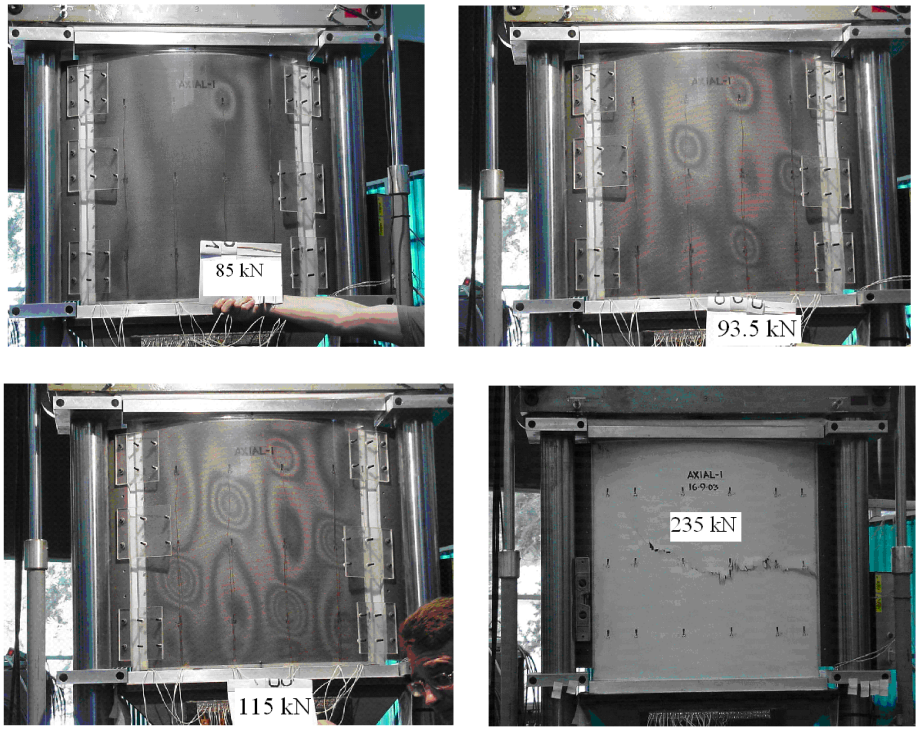

Figure 4. Panel AXIAL1: Development of the buckling pattern as function of axial compression under 85 kN, 93.5 kN, and 115 kN, and after collapse at 235 kN.

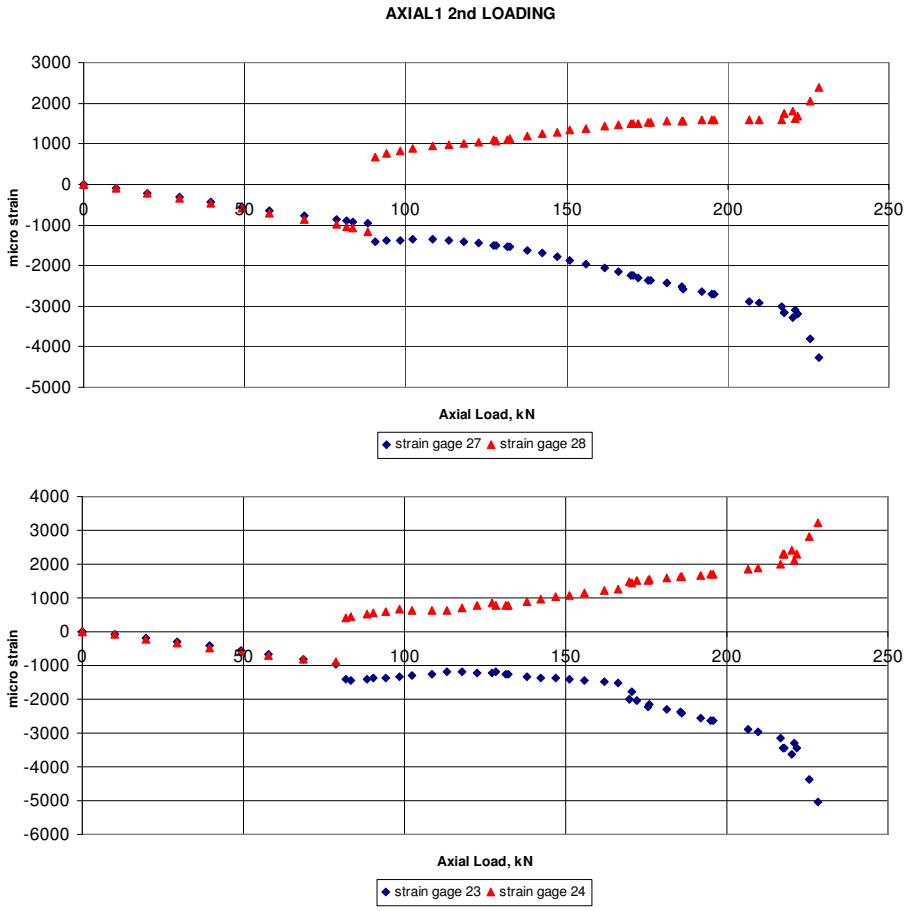

Figure 5. Panel AXIAL1: Strain gage readings versus axial compression.

load was again increased till the panel collapsed at 235.0 kN (Figure 4, bottom right). The collapse was accompanied by breakage of the stringers at mid panel height (across the width of the panel), including the skin.

The second panel tested was AXIAL2. First buckling occurred at 71 kN near gage #19 close to the lower loading end piece (Figure 3). Increase of the axial compression was accompanied by the appearance of more buckling waves (see typical behavior in the first three parts of Figure 6). Typical strain gage readings (gages #15 and 16; see Figure 3) are shown in Figure 7, where the buckling is observed at about 70 kN. The readings of strain gages #27 and 28, at panel mid-height close to the panel supported unloaded edges (see Figure 3), presented in Figure 9, is apparently less definitive. However, careful observation detects local buckling at about 70 kN, in very good agreement with gages 15 and 16. Nine fully developed buckling waves were obtained under 119 kN. The axial loading was increased till 230.5 kN, when collapse occurred (Figure 6, bottom right). Again, collapse was accompanied by breakage of the stringers at the middle of the panel (across the width of the panel), including the skin. Four of the five stringers were broken.

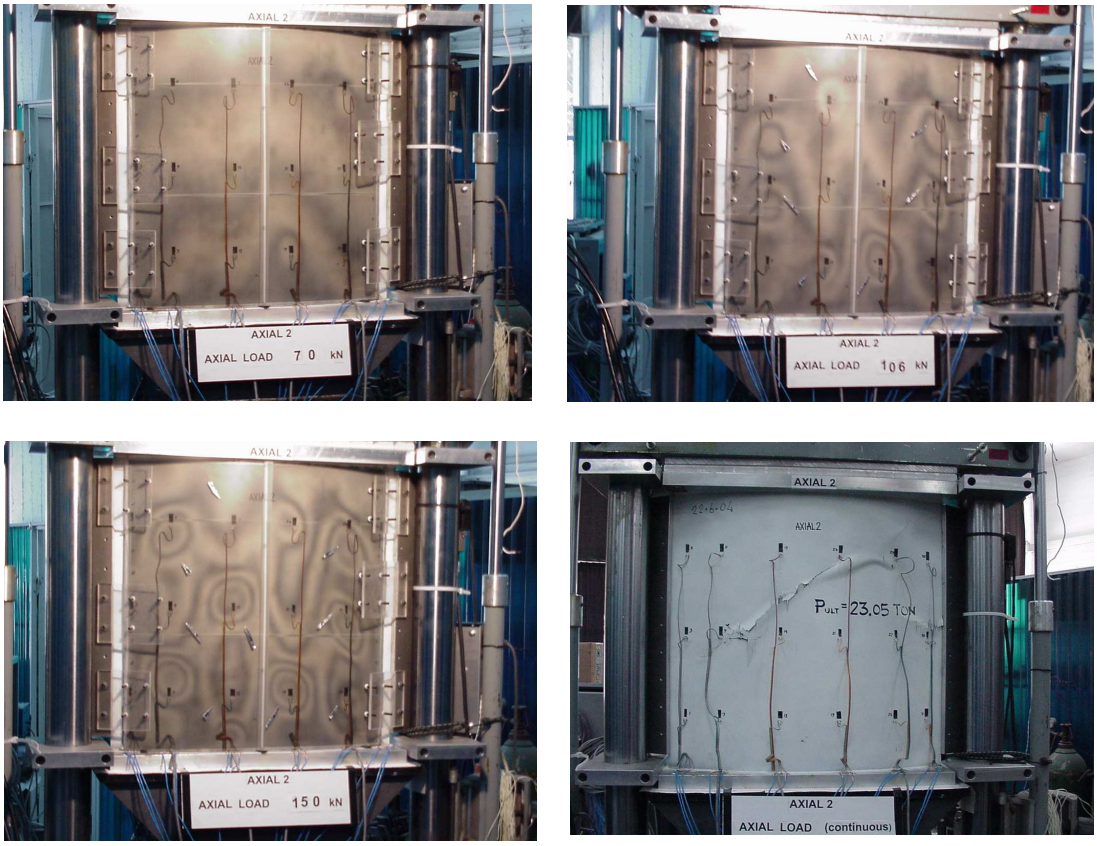

Figure 6. Panel AXIAL2: Development of the buckling pattern as a function of axial compression under 70 kN, 106 kN, 150 kN, and after collapse at 230.5 kN (bottom right).

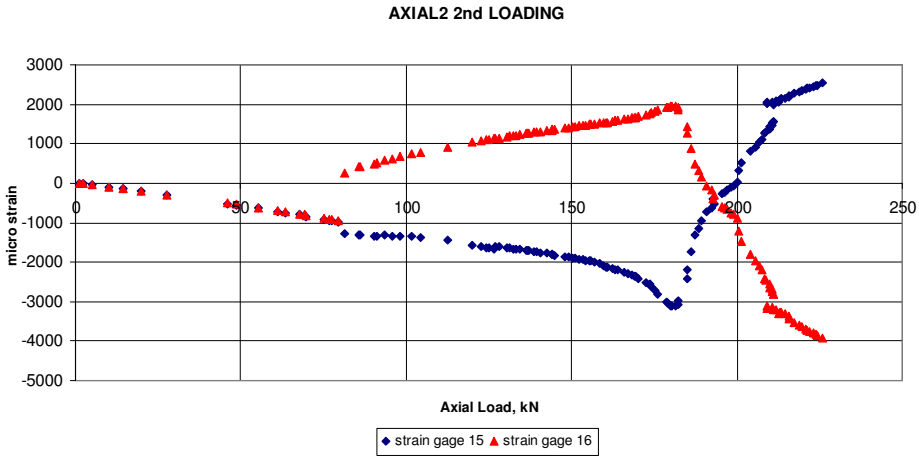

Figure 7a. Panel AXIAL2: Strain gage readings versus axial compression.

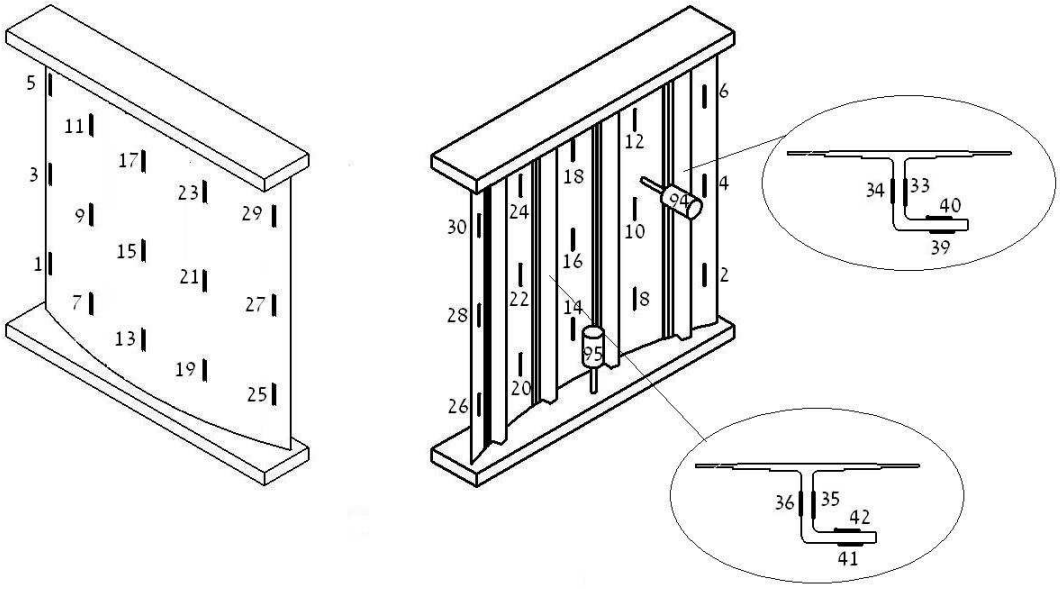

Figure 8. Locations of strain gages and the axial and lateral LVDT's for panels AXIAL3 and AXIAL4.

The third panel tested in the present test series was AXIAL3. It was stiffened by 4 large J-stringers. First buckling occurred at 60 kN with two local waves, one near gage #7, close to the lower loading ,and the other near gage #13, close to the lower loading piece (see Figure 8) and in the bay adjacent to strain gage #7 (Figure 8). Increasing the axial compression led to appearance of more buckling waves (see typical behavior in the first three parts of Figure 9).

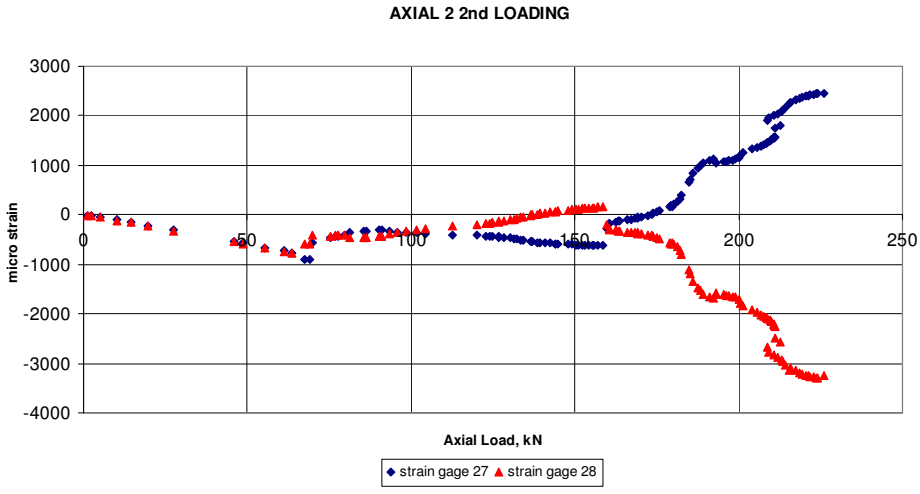

Figure 7b. Panel AXIAL2: Strain gage readings versus axial compression (continued).

Figure 9. Panel AXIAL3: Development of the buckling pattern as a function of axial compression under 65 kN, 125 kN, 190 kN, and after collapse at 295.42 kN (bottom right).

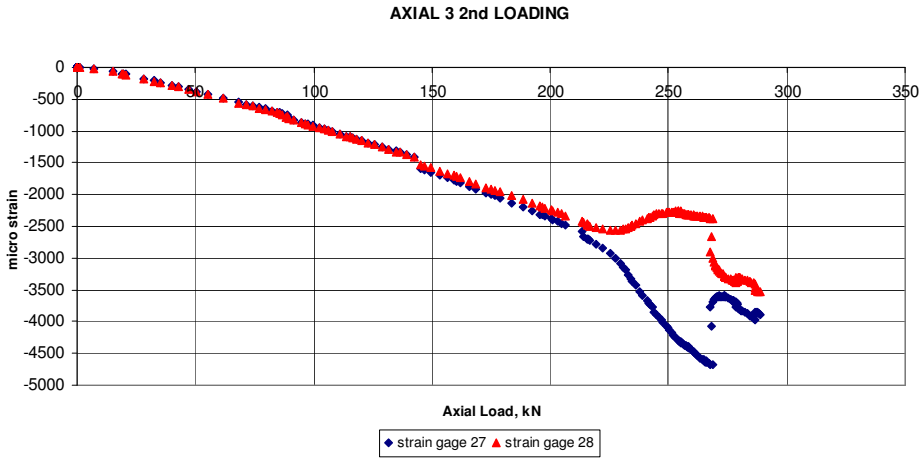

Figure 10. Panel AXIAL3: Strain gages (#27 and 28) readings versus axial compression.

Typical strain gage readings (gages #27 and 28) are shown in Figure 10, where the local buckling load is seen at about 225 kN. Seven fully developed buckling waves were obtained under 164 kN. At a load of 188 kN some noises were noticed, but without visible damage. Noises were also heard under 240 kN and at 280 kN, with the appearance of another wave. The load was further increased till collapse at 295.42 kN (see Figure 9, bottom right) accompanied by a very loud noise. This might indicate a violent failure as compared with a softer failure experienced with the previous panels where such noises were unnoticeable. The collapse was associated with breakage of the stringers in the middle height of the panel (across the width of the panel), separation between the stringers and the skin occurred and the load dropped to 246.0 kN. The panel was held under this load for some time, and then suddenly the load fell again, this time very significantly to 30.0 kN, followed by further damage of the skin.

The last panel tested within the present test series was AXIAL4, a twin of AXIAL3. First buckling occurred at 92.6 kN with two local waves, one near gage #7 close to the lower loading plate and the other near gage #15 at the middle of the panel (Figure 8). Increasing the axial compression caused the appearance of more buckling waves (see typical behavior in the first three parts of Figure 11). Typical strain gage readings (gages #3 and 4) are shown in Figure 12, where local buckling is apparent about

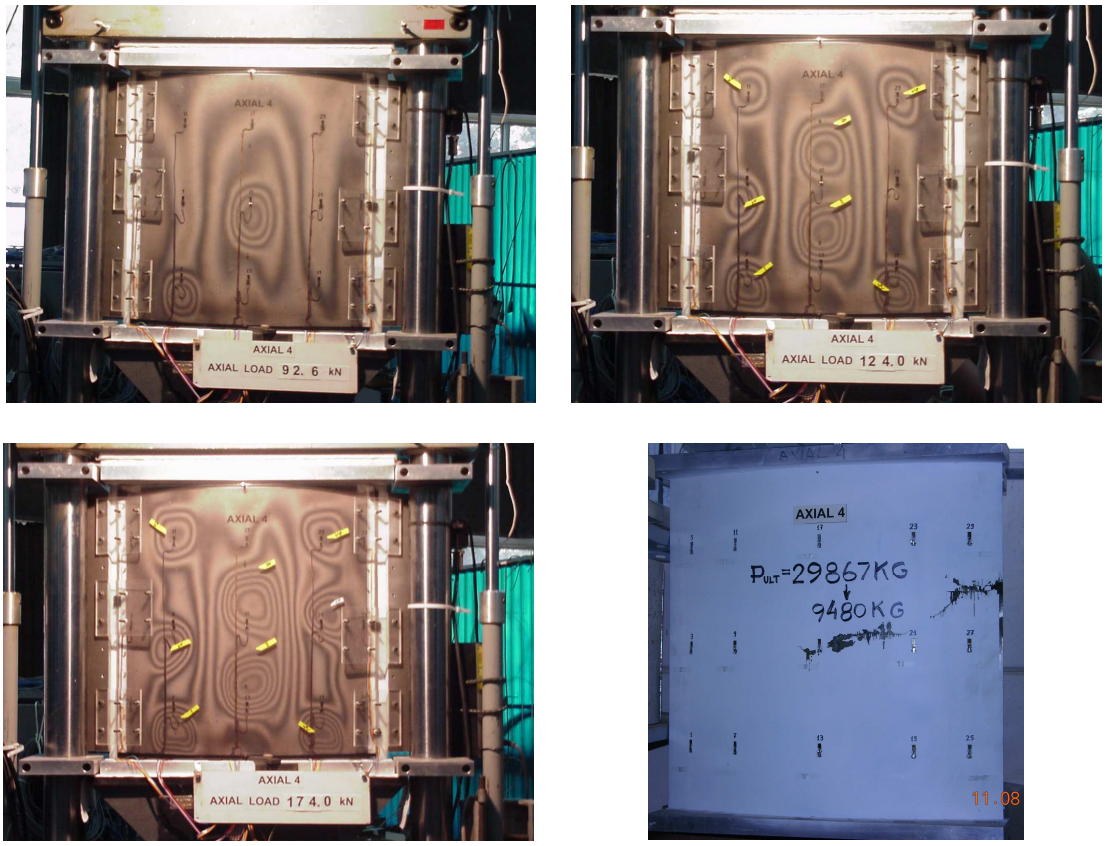

Figure 11. Panel AXIAL4: Development of the buckling pattern as a function of axial compression under 92.6 kN, 124 kN, 174 kN, and after collapse at 298.67 kN.

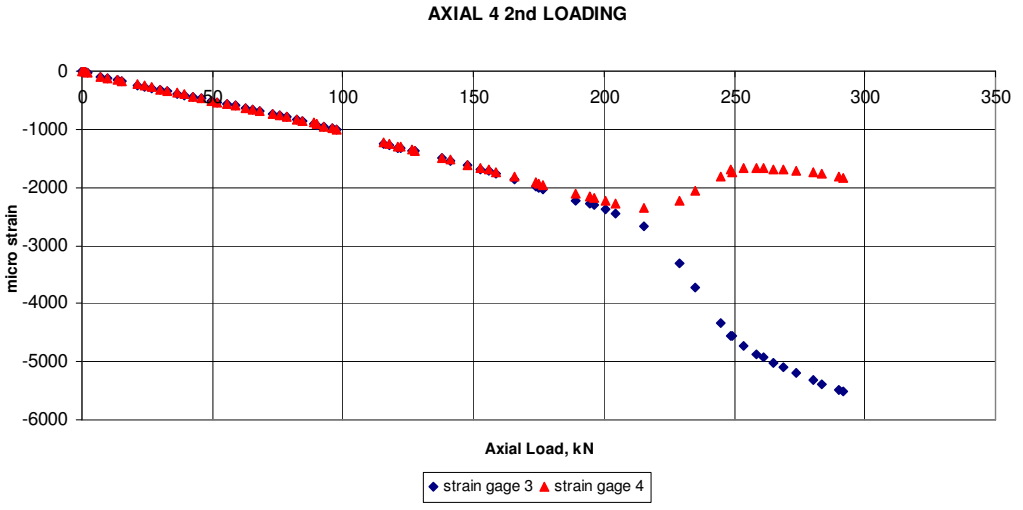

Figure 12. Panel AXIAL4: Strain gages (#3 and 4) readings versus axial compression.

220 kN. Eight fully developed buckling waves were obtained at 174 kN. The load was then increased till collapse of the panel under 298.67 kN (Figure 11, bottom right), again accompanied by a loud noise. The collapse was associated with breakage of the stringers at middle height of the panel (across the width of the panel) including the skin, separation between the stringers and the skin occurred and the axial load dropped to 94.8 kN.

4. Comparisons with calculations

The experimental results obtained in the tests are next compared with numerical analysis using the nonlinear version finite element ABAQUS Explicit [ABAQUS 1998] and the fast tool developed at the Technion, which is based on the effective width method adapted to deal with laminated composite circular cylindrical stringer-stiffened panels [Pevzner et al. 2008].[2] The results are summarized in Table 2 and Figure 13. (ABAQUS/Explicit is a dynamic analysis program; in this case a quasistatic solution is desired, so the prescribed displacement was increased slowly enough to eliminate any significant inertia effect. The displacement was increased linearly using a smooth amplitude function over a time step period of five to ten times longer than the natural period. The collapse load was found using the Riks method.)

The axial stiffness behavior is presented in Figure 13. It shows fair agreement with ABAQUS predictions in the cases of panels AXIAL1 and AXIAL2 (top half of the figure). It is apparent from this figure that the experimental stiffness of the panels observed in the tests is higher than the predicted one. Very good comparison between the experimental results and the calculated stiffness is found in the bottom half of the figure for panels AXIAL3 and AXIAL4.

Determination of the first experimental buckling load is not simple due to the fact that the appearance of a first single buckle during conduct of a test is usually assumed as the first buckling load, as compared with a fully developed pattern of buckles that is numerically predicted (see also detailed discussion in [Abramovich et al. 2008]). Because of this reason the fast tool also overestimates the first experimental

[2]The experimental results of panels AXIAL1–AXIAL4 in Table 1 of [Abramovich et al. 2003] were wrongly reported.

Panel	Experimental		ABAQUS		Effective width method	
	FBL [kN]	CL [kN]	FBL [kN]	CL [kN]	FBL [kN]	CL [kN]
AXIAL1	85.0	235.00	95.0	215.0	100.8	202.6
AXIAL2	71.0	230.50	95.0	215.0	100.8	202.6
AXIAL3	60.0	295.42	75.0	330.0	119.3	354.9
AXIAL4	92.6	298.67	75.0	330.0	119.3	354.9

Table 2. First buckling and collapse loads of panels AXIAL1–AXIAL4: numerical and experimental results using the effective width method [Abramovich et al. 2003] and ABAQUS code run under the assumption of quasistatic behavior. FBL = first buckling load; CL = collapse load.

buckling load by 18.6%–42% in case of the first two panels and by 28.8%–98.8% in case of the last two panels when compared with the experimental results in Table 2. The ABAQUS code overestimates the first buckling load by 11.8%–33.8% in the cases of panels AXIAL1 and AXIAL2. In the cases of panels AXIAL3 and AXIAL4 the code over predicts the first experimental buckling load of panel AXIAL3 by 25% and under predicts by 19% for panel AXIAL4. It appears from Table 2 that there is good agreement between ABAQUS predictions and the fast tool ones in the cases AXIAL1 and AXIAL2 whereas very significant differences exists between the predictions by ABAQUS and the fast tool in the cases AXIAL3 and AXIAL4. Furthermore, ABAQUS predictions are lower in all cases. It is also found from Table 2 that using the fast tool, the experimental collapse loads are under estimated by 12.1%–13.8% in the cases of panels AXIAL1 and AXIAL2 and overestimated by 18.8%–20.0% for panels AXIAL3 and AXIAL4. Employing the ABAQUS code, it is seen in Table 2 that the collapse loads are underestimated by 8.5%–6.7% for panels AXIAL1 and AXIAL2, and overestimated by 11.7%–10.5% in the cases AXIAL3 and AXIAL4.

Table 2 reveals good agreement between ABAQUS and the fast tool predictions of the collapse loads. In the cases AXIAL1 and AXIAL2, stiffeners with smaller flange, both codes predict collapse loads that are lower than those experienced in the tests. Also, ABAQUS predictions are higher than those yielded by the fast tool. On the other hand, in the cases AXIAL3 and AXIAL4, stiffeners with larger flanges, both codes predict higher collapse loads than those observed experimentally. However, in this case the ABAQUS predictions are lower than those obtained by the fast tool.

5. Formulation of design rules

Based on the experimental effort carried out within the framework of the POSICOSS project and reported in [Abramovich et al. 2003; 2008], as well as in the present study, and employing the fast tool [Pevzner et al. 2008], design guidelines are next formulated and presented (Table 3).

Figures 14 and 15 present the skin buckling and collapse loads of the tested panels versus the parameter $b/\sqrt{R \cdot s}$, a nondimensional parameter commonly employed in shell analysis to describe the influence of shell radius R, its thickness s, and the distance between the stringers b. It is evident from Figure 14 that as the distance b between two adjacent stringers increases, the first skin buckling load decreases. Panels PSC7–PSC9 demonstrated the highest buckling loads (the panels have 6 blade stringers each),

while as expected, panels AXIAL3 and AXIAL4, each with 4 J-type stringers, experienced the lowest values. The decrease in first buckling is much emphasized in the blade-stiffened panels, whereas in the case of the J-stiffened panels barely exists.

It appears from Figure 15 that either increasing the number of the stringers or their cross-section would yield a higher collapse load of a panel under axial compression. This is apparent for panels AXIAL3 and AXIAL4 (each having 4 J-type stringers with a wide flange) and panels PSC7–PSC9 (each having 6 blade stringers). The parameter $b/\sqrt{R \cdot s}$ does not influence the collapse load in a consistent manner, since there is more than one degree of freedom that can raise the collapse load. Nevertheless, it is observed that in the case of blade-stiffened panels, collapse decreases with increase in $b/\sqrt{R \cdot s}$, whereas the opposite is found for the J-stiffened panels.

The ratio of the collapse load to the corresponding first buckling load, the skin buckling, versus $b/\sqrt{R \cdot s}$ is presented in Figure 15, right. It is seen that the PSC panels, which are stiffened by blade type

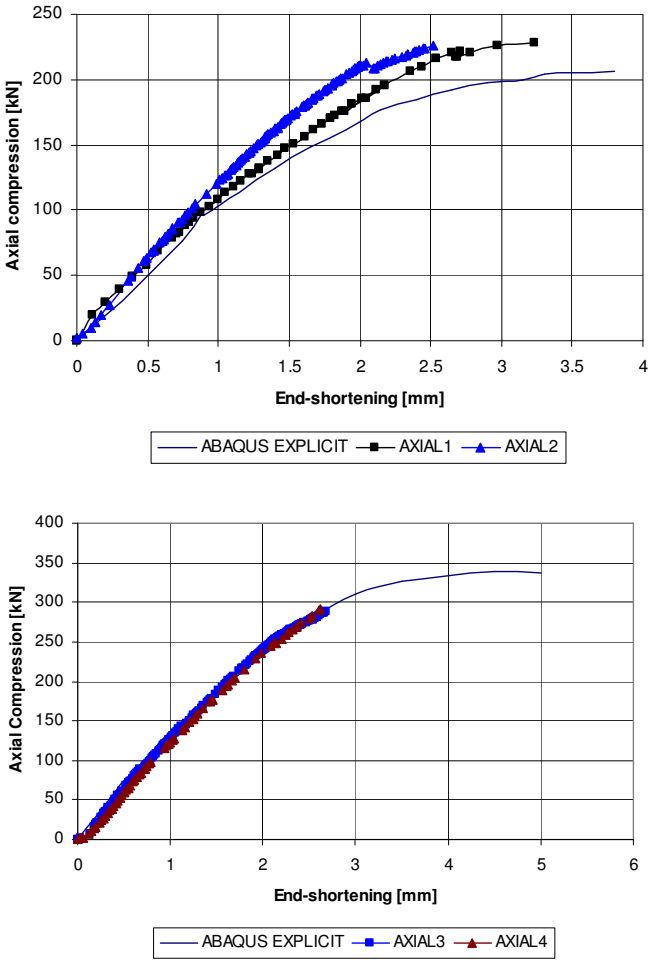

Figure 13. Axial compression versus end shortening: numerical and experimental results. Top: panels with with small J-stiffener; bottom: panels with large J-stiffener.

Panel	h_s [mm]	Stringers	FBL [kN]	CL [kN]	$\sum m_i$ [kg]	$\left(\sum m_i\right)/M$
AXIAL1	20.5	5 Small J	85.0	235.00	0.7656	0.516014
AXIAL2	20.5	5 Small J	71.0	230.50	0.7656	0.516014
AXIAL3	20.5	4 Big J	60.0	295.48	0.9293	0.564103
AXIAL4	20.5	4 Big J	92.6	298.67	0.9293	0.564103
BOX1 (panel A)	20	5 Blade	120.3	–	0.8448	0.540541
BOX1 (panel B)	20	5 Blade	134.0	–	0.8448	0.540541
BOX2 (panel A)	20	5 Blade	115.5	–	0.8448	0.540541
BOX2 (panel B)	20	5 Blade	–	–	0.8448	0.540541
BOX3 (panel A)	20.5	5 Small J	79.0	–	0.7656	0.516014
BOX3 (panel B)	20.5	5 Small J	100.0	–	0.7656	0.516014
BOX4 (panel A)	20.5	4 Big J	57.5	–	0.9293	0.564103
BOX4 (panel B)	20.5	4 Big J	57.5	–	0.9293	0.564103
PSC1	20	5 Blade	131.0	212.7	0.8448	0.54054
PSC2	20	5 Blade	150.0	227.0	0.8448	0.54054
PSC4	20	5 Blade	158.5	229.2	0.8448	0.54054
PSC3	15	5 Blade	136.0	162.0	0.6336	0.46875
PSC5	15	5 Blade	113.0	152.6	0.6336	0.46875
PSC6	15	5 Blade	126.0	140.0	0.6336	0.46875
PSC7	20	6 Blade	228.5	228.5	1.0138	0.58537
PSC8	20	6 Blade	240.0	240.0	1.0138	0.58537
PSC9	20	6 Blade	244.0	244.0	1.0138	0.58537

Table 3. First buckling loads (FBL) and collapse loads (CL) found in experimental tests reported in this article and in [Abramovich et al. 2003; 2008].

stringers, experience a consistent and almost constant ratio of 1.125–1.624, whereas the panels AXIAL1–AXIAL4, stiffened by J-type stringers, exhibit significantly higher ratios, in the range of 3.225–4.925, that increase significantly with increase in stiffener cross-section.

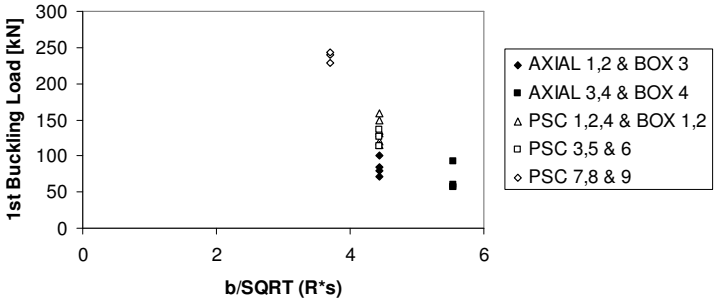

Figure 14. Skin buckling loads of the tested panels versus $b/\sqrt{R \cdot s}$. For all panels, $R = 938$ mm and $s = 1$ mm.

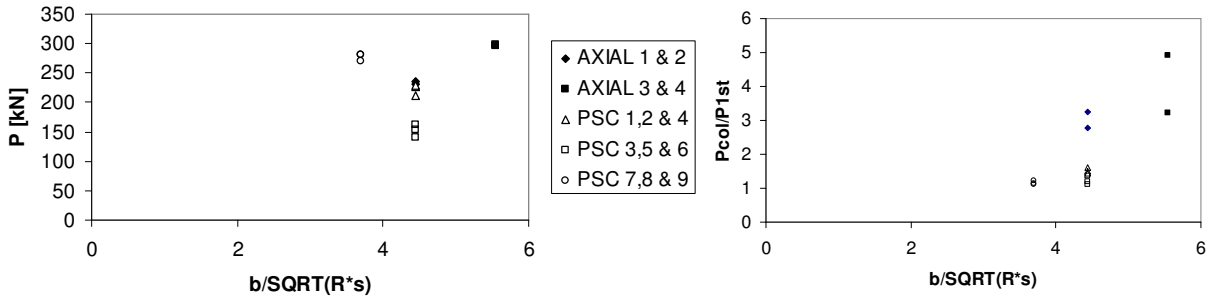

Figure 15. Collapse load (left) and ratio between collapse load and skin buckling load (right) for the tested panels versus $b/\sqrt{R \cdot s}$. Recall that $R = 938$ mm and $s = 1$ mm.

Considering from a design point of view the results presented in Figures 14 and 15 it may be concluded that the simpler and cheaper blade-stiffened panels are superior to the J-type ones when design is based on first skin buckling. However, this argument prevails provided these blade-stiffened panels exhibit a wide enough range to withstand postbuckling. The condition imposed is that the collapse loads corresponding to these type of panels meet the design requirement, namely an ultimate load equal at least to one and a half times the limit load, which according to the present adopted design approach equals the first buckling load. It appears from Table 3 and Figure 15, right, that only the blade stiffened panels PSC1, PSC2, and PSC4 barely meet this condition. On the other hand, when considering the postbuckling capacity of the J-stiffened panels it is apparent from the same table and figure that they possess a very wide range of postbuckling carrying capacity that is associated with collapse loads equal to many times their first skin buckling. It should be noted (see Table 3 and Figure 14), and as already mentioned, that their first skin buckling is low, as a matter of fact the lowest experienced among the panels tested in the present program. Obviously, these observations contradict the low weight low cost demands, the J-stiffened panels are relatively heavy and their manufacturing is complex and more expensive.

In the preceding figures the mass of the panels has been ignored. Obviously, their specific load carrying capacities are the appropriate measures to evaluate their performances. Hence, the panel mass is taken into account and the corresponding results are presented in Figures 16 and 17 for the skin and the collapse loads, respectively. Also in presenting the results, the stringer area is taken into account: instead of using the parameter $b/\sqrt{R \cdot s}$, we use $b/\sqrt{R \cdot s_1}$, where s_1 is defined as

$$s_1 = s\left(1 + \frac{A}{b \cdot s}\right). \tag{1}$$

Here A is the area of the stringer, b is the distance between stringers, and s is the skin thickness. This modified parameter is commonly used when dealing with stringer-stiffened shells and it is therefore also adopted for the present stringer-stiffened panels (it represents a shell/panel with an equivalent uniform skin where the stiffeners are smeared).

Considering the specific first buckling, the behavior observed earlier for both stiffener types in Figure 14 is again exhibited in Figure 16, the highest specific first skin buckling loads are associated with the minimum distance between stringers. As found in Figure 14, the blade stiffened panels (PSC7, PSC8,

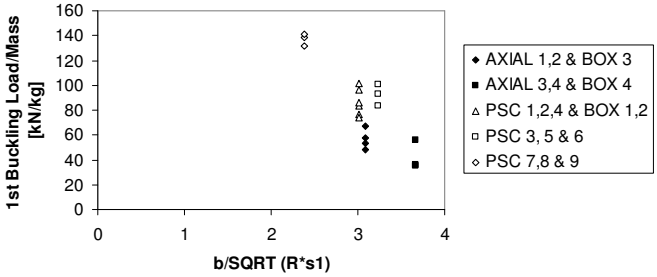

Figure 16. Specific skin buckling loads of the tested panels versus $b/\sqrt{R \cdot s_1}$, where s_1 is given by Equation (1).

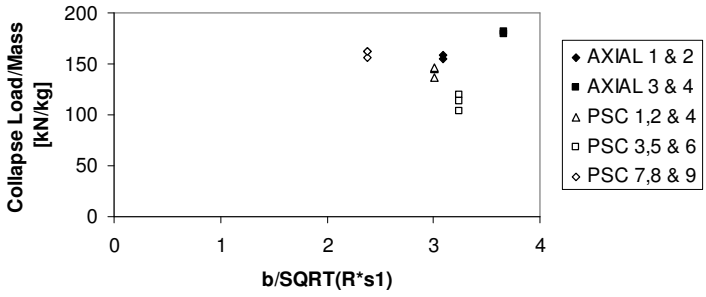

Figure 17. Specific collapse loads of the tested panels versus $b/\sqrt{R \cdot s_1}$.

and PSC9) yield the higher specific first buckling loads. The detailed observations and results shown in Figure 16 are similar to those pertinent to Figure 14; thus the discussion of Figure 14 applies to Figure 16 as well.

Figure 17 shows that when considering specific collapse loads versus $b/\sqrt{R \cdot s_1}$, as in Figure 15, the panels with either the larger stiffeners cross section (AXIAL3 and AXIAL4) or with the larger number of stringers (6 stringers, panels PSC7–PSC9) yield the higher specific collapse values. The worst observation was experienced with panels PSC3, PSC5, and PSC6 (5 stringers with a height of 15 mm). Increasing the blade stiffeners height to $h = 20$ mm (panel PSC1, PSC2, and PSC4) increased the panel specific collapse load, almost to that corresponding to panels AXIAL1 and AXIAL2. It is observed in Figure 17 that the specific collapse loads of panels AXIAL1 and AXIAL2 are almost identical with those of panels PSC7–PSC9. Hence, the specific collapse loads of panels PSC1, PSC2, and PSC4 are quite comparable with those of PSC7–PSC9. Consequently, from a design point of view the simpler and cheaper blade-stiffened configuration presents and provides a much more attractive and favorable configuration for sustaining a prescribed specific collapse load. However, as already discussed above, this holds only when the design meets the required ratio between the limit and ultimate loads.

Next a parametric investigation was performed to calculate the collapse loads of various configurations of panels stiffened by blade and small J-type stringers using the fast tool [Pevzner et al. 2008]. Two J-types of stringers were used, one with 18 layers (thickness of 2.25 mm), and a small flange of 10 mm long and the other having 24 layers (thickness of 3 mm) and a small flange of 10 mm. The height of the stringers was 20.5 mm. The blade type stringers had 24 layers (thickness of 3.0 mm) and two heights 15

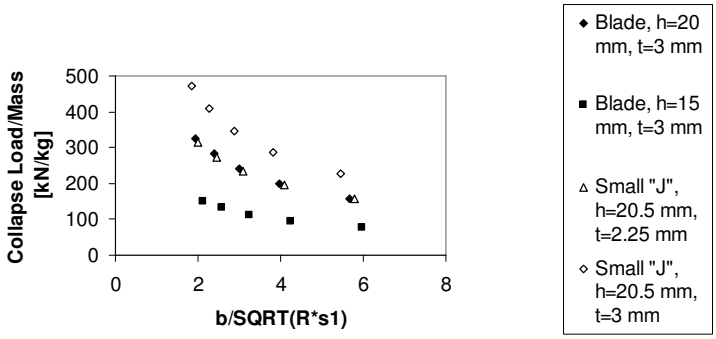

Figure 18. Specific collapse loads predicted by the effective width method for the tested panels, versus $b/\sqrt{R \cdot s_1}$.

and 20 mm. The distances between the stringers, b, were: 226.67, 170.0, 136.0, 113.3, and 97.1 mm, corresponding to 3, 4, 5, 6, and 7 stringers per panel, respectively.

The calculated results are presented in Figure 18. It is observed in this figure that a relatively small increase in J-stiffener dimensions increases significantly their specific collapse load. On the other hand, a more noticeable change in blade stiffeners dimensions is required to achieve a noticeable increase in their specific collapse load capacity. However, by introducing changes in the blades height the specific collapse load capacities of the blade-stiffened panels become equal to those corresponding to the J-stiffened ones. As already discussed above, this makes the blade-stiffened panels more attractive and preferable from a design point of view.

6. Derivation of design guidelines

- Results of analyses show that the influence of panel length on skin buckling load can be neglected within the design space ($400\,\text{mm} \leq l \leq 800\,\text{mm}$).[3]
- The influence of panel length on the collapse load is significant as long as local instability does not coincide with general instability. Like in a column, the collapse load significantly decreases with increase in panel length. There is a significant influence of the panel length on the ratio of its collapse load to its skin buckling load.
- Assuming that the total length of the structure is fixed, an increase of the collapse load can be achieved by introduction of additional frames. This results in a corresponding increase of the weight of the structure.
- In general, decrease in the stringer spacing leads to increase of skin buckling as well as of the collapse load. Assuming that the total arc-length of a structure is fixed, a decrease in the stringer spacing means more stringers and increase of the collapse load. In this case the weight of the

[3]Not all of the design guidelines presented herein stem directly from the results presented in the present manuscript but were derived to reflect all the partners' results of the POSICOSS project to enable a wider use. See [Zimmermann and Rolfes 2006; Bisagni and Cordisco 2006; Zimmermann et al. 2006; Lanzi and Giavotto 2006; Möcker and Reimerdes 2006; Rikards et al. 2006].

structure is increased in proportion to the increase of the number of stiffeners but not the specific collapse load. Regarding the influence of the stringer spacing on the ratio of collapse load to first skin buckling load, no general tendency can be observed from the results of the experimental and parametric studies. Based on the experimental observations reported in Figure 15, right, it appears that almost no effect on the ratio was experienced with blade stiffened panels, whereas a very strong effect was found in the case of J-stiffened panels.

- As a general result of analyses it can be pointed out that skin buckling load per unit length is increased when the panel radius is reduced. Regarding the influence of the radius on the collapse load, an increase of the collapse load was found when reducing the radius. However, in most designs the radius will be fixed and thus the influences of this parameter cannot be exploited to improve the design.
- As a common result of analyses one can summarize that the skin buckling load per unit length is increased when the stringer geometry dimensions are increased. This holds till one reaches values of dimensions of the stringer for which it represents a clamped boundary condition. Therefore, it is not recommended to increase the dimensions of the stringer beyond this value. The collapse load of blade-stiffened panels increases when the stringer height is increased from $h = 14\,\text{mm}$ to $h = 20\,\text{mm}$, but further increase from $h = 20\,\text{mm}$ to $h = 30\,\text{mm}$ leads to reduction of the collapse load. This is caused by a change of the type of instability experienced when increasing the stringer height. While buckling of the stringers in bending leads to the collapse of the $h = 20\,\text{mm}$ stringers, collapse is caused by torsional buckling in case of the $h = 30\,\text{mm}$ stringers. Furthermore, it should be remembered in design of blade-stiffened panels that an increase of stringer height may lead to decrease of the local buckling load of the stringer. Therefore, it has to be ensured that local buckling of the stringer is avoided before global buckling of the panel. Within the design space that was defined for the present parametric studies this problem was not encountered, but it might be crucial in the case of thin and long stringer blades. Regarding the panel weight, it can be pointed out that increase of the stringer dimensions leads to a relatively small increase (proportional to the additional weight) of the panel weight, provided that the type of the stringer is kept constant.
- Considering the specific collapse load (the ratio of the collapse load over the mass of the panel) versus the modified parameter $b/\sqrt{R * s_1}$ presents a more realistic presentation, because it takes into consideration the cross-section of the stringers, or rather the equivalent skin thickness of the panel.
- There is no advantage in application of J-type stringers over the common practice blade types. There is no gain in local buckling, whereas the significant increase in the collapse load of J-stiffened panels cannot be exploited and thus there is a considerable weight penalty. Due to manufacturing and cost constraints, the blade-stiffener would be the ideal and preferred stringer to stiffen a curved panel.

7. Conclusions

Test results on curved composite panels stiffened by J-stringers were presented and discussed. Test results were compared with predictions yielded by an in-house developed code and the commercial FE code ABAQUS, as well as with test results on blade-stiffened panels that were reported earlier. Design

guidelines have been formulated based on the Technion experimental results and the fast in-house software tool developed within the POSICOSS program. Test results and calculations have demonstrated that from a design point of view, weight reduction, and cost, blade type stringers are more favorable. The design guidelines would allow the designer to better choose a panel configuration to meet prescribed design requirements with various optimisations leading to a higher specific load capacity.

Acknowledgment

We thank Mr. A. Grunwald and Mrs. R. Yaffe, Aerospace Structures Laboratory, Technion, Haifa, Israel for their exceptional assistance in setting up the tests and dedicated assistance in performing them. We also thank Dr. P. Pevzner of the same laboratory for his helpful assistance in carrying out the numerical calculations.

References

[ABAQUS 1998] *ABAQUS/Explicit: keywords version*, Hibbitt, Karlsson and Sorensen, Pawtuckett, RI, 1998.

[Abramovich et al. 2003] H. Abramovich, A. Grunwald, P. Pevsner, T. Weller, A. David, G. Ghilai, A. Green, and N. Pekker, "Experiments on axial compression postbuckling behavior of stiffened cylindrical composite panels", in *44th AIAA/ASME/ASCE/AHS/ASC Structures, Structural Dynamics, and Materials Conference* (Norfolk, VA, 2003), AIAA, Reston, VA, 2003. Paper #2003-1793.

[Abramovich et al. 2008] H. Abramovich, T. Weller, and C. Bisagni, "Buckling behavior of composite laminated stiffened panels under combined shear-axial compression", *J. Aircraft* **45**:2 (2008), 402–413.

[Bisagni and Cordisco 2006] C. Bisagni and P. Cordisco, "Post-buckling and collapse experiments of stiffened composite cylindrical shells subjected to axial loading and torque", *Compos. Struct.* **73**:2 (2006), 138–149.

[Bucci and Mercuria 1992] A. Bucci and U. Mercuria, "CFRP stiffened-panels under compression", pp. 12.1–12.14 in *The utilization of advanced composites in military aircraft* (San Diego, CA, 1991), AGARD Report **785**, AGARD/NATO, Neuilly-sur-Seine, 1992.

[Card 1966] M. F. Card, "Experiments to determine the strength of filament-wound cylinders loaded in axial compression", Technical Note TN D-3522, NASA, Washington, DC, 1966, Available at http://hdl.handle.net/2060/19660023039.

[Degenhardt et al. 2006] R. Degenhardt, R. Rolfes, R. Zimmermann, and K. Rohwer, "COCOMAT: improved material exploitation at safe design of composite airframe structures by accurate simulation of collapse", *Compos. Struct.* **73**:2 (2006), 175–178.

[Frostig et al. 1991] Y. Frostig, G. Siton, A. Segal, I. Sheinman, and T. Weller, "Postbuckling behavior of laminated composite stiffeners and stiffened panels under cyclic loading", *J. Aircraft* **28**:7 (1991), 471–480.

[Hutchinson and Koiter 1970] J. W. Hutchinson and W. T. Koiter, "Postbuckling theory", *Appl. Mech. Rev.* (*ASME*) **23** (1970), 1353–1366.

[Johnson 1978] R. Johnson, Jr., "Design and fabrication of a ring-stiffened graphite-epoxy corrugated cylindrical shell", Contractor Report CR-3026, NASA, Washington, DC, 1978, Available at http://hdl.handle.net/2060/19780023522.

[Knight and Starnes 1988] N. F. Knight, Jr. and J. H. Starnes, Jr., "Postbuckling behavior of selected curved stiffened graphite-epoxy panels loaded in axial compression", *AIAA J.* **26**:3 (1988), 344–352.

[Lanzi and Giavotto 2006] L. Lanzi and V. Giavotto, "Post-buckling optimization of composite stiffened panels: computations and experiments", *Compos. Struct.* **73**:2 (2006), 208–220.

[Lei and Cheng 1969] M. M. Lei and S. Cheng, "Buckling of composite and homogeneous isotropic cylindrical shells under axial and radial loading", *J. Appl. Mech.* (*ASME*) **36** (1969), 791–798.

[Lilico et al. 2002] M. Lilico, R. Butler, G. W. Hunt, A. Watson, D. Kennedy, and F. W. Williams, "Analysis and testing of a postbuckled stiffened panel", *AIAA J.* **40**:5 (2002), 996–1000.

[Möcker and Reimerdes 2006] T. Möcker and H.-G. Reimerdes, "Postbuckling simulation of curved stiffened composite panels by the use of strip elements", *Compos. Struct.* **73**:2 (2006), 237–243.

[Pevzner et al. 2008] P. Pevzner, H. Abramovich, and T. Weller, "Calculation of the collapse load of an axially compressed laminated composite stringer-stiffened curved panel: an engineering approach", *Compos. Struct.* **83** (2008), 341–353.

[Rikards et al. 2006] R. Rikards, H. Abramovich, K. Kalnins, and J. Auzins, "Surrogate modeling in design optimization of stiffened composite shells", *Compos. Struct.* **73**:2 (2006), 244–251.

[Romeo 1986] G. Romeo, "Experimental investigation on advanced composite-stiffened structures under uniaxial compression and bending", *AIAA J.* **24**:11 (1986), 1823–1830.

[Segal et al. 1987] A. Segal, G. Siton, and T. Weller, "Durability of graphite-epoxy stiffened panels under cyclic postbuckling compression loading", pp. 5.69–5.78 in *ICCM and ECCM: 6th International Conference on Composite Materials and 2nd European Conference on Composite Materials* (London, 1987), edited by F. L. Matthews et al., Elsevier, London, 1987.

[Singer et al. 2002] J. Singer, J. Arbocz, and T. Weller, *Buckling experiments: experimental methods in buckling of thin-walled structures*, vol. 2, Wiley, New York, 2002.

[Sobel and Agarwal 1976] L. H. Sobel and B. L. Agarwal, "Buckling of eccentrically stringer-stiffened cylindrical panels under axial compression", *Comput. Struct.* **6**:3 (1976), 193–198.

[Starnes et al. 1985] J. H. Starnes, Jr., N. F. Knight, Jr., and M. Rouse, "Postbuckling behavior of selected flat stiffened graphite-epoxy panels loaded in compression", *AIAA J.* **23**:8 (1985), 1236–1246.

[Tennyson et al. 1972] R. C. Tennyson, D. B. Muggeridge, K. H. Chan, and N. S. Khot, "Buckling of fiber-reinforced circular cylinders under axial compression", Technical Report TR-72-102, Air Force Flight Dynamics Laboratory, Wright–Patterson Air Force Base, OH, 1972.

[Vestergen and Knutsson 1978] P. Vestergen and L. Knutsson, "Theoretical and experimental investigation of the buckling and postbuckling characteristics of flat carbon fiber reinforced plastic (CFRP) panels subjected to compression or shear loading", pp. 217–223 in *Proceedings of the 11th Congress of the International Council of the Aeronautical Sciences* (*ICAS*) (Lisbon, 1978), edited by J. Singer and R. Staufenbiel, Mirandela, Lisbon, 1978.

[Zimmermann and Rolfes 2006] R. Zimmermann and R. Rolfes, "POSICOSS: improved postbuckling simulation for design of fibre composite stiffened fuselage structures", *Compos. Struct.* **73**:2 (2006), 171–174.

[Zimmermann et al. 2006] R. Zimmermann, H. Klein, and A. Kling, "Buckling and postbuckling of stringer stiffened fibre composite curved panels: tests and computations", *Compos. Struct.* **73**:2 (2006), 150–161.

Received 15 Nov 2008. Revised 23 Feb 2009. Accepted 24 Feb 2009.

HAIM ABRAMOVICH: haim@aerodyne.technion.ac.il
Faculty of Aerospace Engineering, Technion – Israel Institute of Technology, 32000 Haifa, Israel
http://ae-www.technion.ac.il/

TANCHUM WELLER: tanchum@aerodyne.technion.ac.il
Faculty of Aerospace Engineering, Technion – Israel Institute of Technology, 32000 Haifa, Israel
http://ae-www.technion.ac.il/